



**HAL**  
open science

# **In vitro digestion of foods using pH-stat and the INFOGEST protocol: Impact of matrix structure on digestion kinetics of macronutrients, proteins and lipids**

Damien J L Mat, Steven Le Feunteun, Camille Michon, Isabelle Souchon

## **► To cite this version:**

Damien J L Mat, Steven Le Feunteun, Camille Michon, Isabelle Souchon. In vitro digestion of foods using pH-stat and the INFOGEST protocol: Impact of matrix structure on digestion kinetics of macronutrients, proteins and lipids. Food Research International, 2016, 88, pp.226-233. <10.1016/j.foodres.2015.12.002>. <hal-01384421>

**HAL Id: hal-01384421**

**<https://hal.science/hal-01384421v1>**

Submitted on 15 May 2025

**HAL** is a multi-disciplinary open access archive for the deposit and dissemination of scientific research documents, whether they are published or not. The documents may come from teaching and research institutions in France or abroad, or from public or private research centers.

L'archive ouverte pluridisciplinaire **HAL**, est destinée au dépôt et à la diffusion de documents scientifiques de niveau recherche, publiés ou non, émanant des établissements d'enseignement et de recherche français ou étrangers, des laboratoires publics ou privés.



HAL Authorization

1 This file presents the 'accepted version' of the following original research article:  
2 *Mat, D. J. L., Le Feunteun, S., Michon, C., & Souchon, I. (2016). In vitro digestion of foods*  
3 *using pH-stat and the INFOGEST protocol: Impact of matrix structure on digestion kinetics of*  
4 *macronutrients, proteins and lipids. Food Research International, 88, 226–233.*  
5 <https://doi.org/10.1016/j.foodres.2015.12.002>

6

7

8 ***In vitro* digestion of foods using pH-stat and the INFOGEST protocol:**  
9 **Impact of matrix structure on digestion kinetics of macronutrients, proteins**  
10 **and lipids**

11 Damien J. L. Mat<sup>a,b,c,d</sup>, Steven Le Feunteun<sup>a,b\*</sup>, Camille Michon<sup>c,d</sup> and Isabelle Souchon<sup>a,b</sup>

12 <sup>a</sup> AgroParisTech, UMR782 Génie et Microbiologie des Procédés Alimentaires, F-78850 Thiverval

13 Grignon

14 <sup>b</sup> INRA, UMR782 Génie et Microbiologie des Procédés Alimentaires, F-78850 Thiverval Grignon

15 <sup>c</sup> AgroParisTech, UMR1145 Ingénierie Procédés Aliments, 1 rue des Olympiades, F-91300 Massy

16 <sup>d</sup> INRA, UMR1145 Ingénierie Procédés Aliments, 1 rue des Olympiades, F-91300 Massy

17 \* Corresponding author: [steven.le-feunteun@grignon.inra.fr](mailto:steven.le-feunteun@grignon.inra.fr)

18 **Abstract**

19 It is currently admitted that food structure can facilitate or delay the release of nutrients during digestion  
20 and their absorption by the Human body. The aim of this study is to propose an *in vitro* method able to  
21 assess the behavior of lipo-proteinic matrices with different structures during digestion. Two model  
22 matrices of exactly the same compositions (10 % oil, 15 % whey proteins, w/w) were designed: i) A  
23 liquid emulsion (LE) made of small fat droplets (1  $\mu\text{m}$ ) dispersed in a liquid continuous phase containing  
24 native whey proteins, ii) A solid emulsion (SE) made of a continuous whey protein gel entrapping large  
25 oil droplets (20  $\mu\text{m}$ ). The two matrices were digested through an *in vitro* gastro-intestinal protocol based  
26 on the INFOGEST guidelines using pH-stat to monitor the enzymatic hydrolyses of both proteins and  
27 lipids. By further digesting lipid-free matrices in the same conditions, the contributions of the proteolytic  
28 and lipolytic reactions were evaluated. Significant differences were observed between matrices at both  
29 short and long digestion times. The initial rates of both proteolysis and lipolysis were slower for SE than  
30 LE because of the gel state of the continuous phase. At the end of the experiments, SE led to a smaller  
31 extent of lipolysis ( $\text{DH}_{\text{lip\_SE}} = 51 \% < \text{DH}_{\text{lip\_LE}} = 81 \%$ ) but a greater extent of proteolysis ( $\text{DH}_{\text{prot\_SE}} = 80$   
32  $\% > \text{DH}_{\text{prot\_LE}} = 52 \%$ ) because of the higher sensitivity to digestion of denatured whey proteins. These  
33 results highlight the impact of matrix structure on enzyme accessibility, and show that the proposed  
34 method is suitable to monitor the digestion of complex food matrices.

35 **Key words:** Food structure; Gastro-intestinal digestion; Pancreatin; Lipolysis; Proteolysis;  
36 Emulsion gel.

37

38 **Abbreviations**

39 WPI: whey protein isolate; WP: whey proteins; FFA: free fatty acids; SSF: simulated salivary fluid;  
40 eSSF: electrolyte mix in the SSF; SGF: simulated gastric fluid; eSGF: electrolyte mix in the SGF; SIF:  
41 simulated intestinal fluid; eSIF: electrolyte mix in the SIF; LE: liquid proteinic emulsion-type matrix;  
42 LCP liquid proteinic continuous phase matrix; SE: solid proteinic emulsion-type matrix; SCP: solid  
43 proteinic continuous phase matrix; DH: degree of hydrolysis.

## 44 **1 Introduction**

45 It is now well-established that food structure can facilitate or limit the release and subsequent  
46 metabolization of nutrients. Understanding how food structure can modulate digestion kinetics and/or  
47 macronutrient digestibility has therefore become a main issue, which may lead to more-effective ways  
48 of maintaining a healthy diet. Knowledge on the food structure-physiology interactions may indeed be  
49 useful when considering the effects of particular diets and consumption habits, but also to design foods  
50 targeted for specific health functionalities (J. E. Norton, Wallis, Spyropoulos, Lillford, & Norton, 2014).

51 Food in the human digestive tract is subject to chemical-physics transformations while passing through  
52 the different compartments. In the stomach, gastric secretions contain hydrochloric acid decreasing the  
53 pH to the 1-5 range (Guerra et al., 2012), as well as gastric lipase and pepsin which initiate the lipolytic  
54 and proteolytic reactions, respectively. In the case of solid food, the fragments are progressively grinded  
55 until their size is reduced enough to pass into the proximal part of the small intestine, the duodenum. In  
56 the small intestine, pH progressively rises to about 7, while the enzymes secreted in the pancreatic juice  
57 continue the hydrolysis of macronutrients. Pancreatic lipase, in association with its co-lipase, bile acids  
58 and other lipases perform lipolysis (H. Singh, Ye, & Horne, 2009), while proteases, such as trypsin and  
59 chymotrypsin, perform proteolysis (Mackie & Macierzanka, 2010; Turgeon & Rioux, 2011). The  
60 hydrolysis of lipids and of proteins is considered almost complete at the end of the small intestine.

61 *In vitro* gastrointestinal digestion experiments have proved to be a powerful means to gain knowledge  
62 on the nutritional value of foods as they allow condition controlling and easy sampling (Guerra et al.,  
63 2012). Although the capacity of *in vitro* approaches to mimic the physiological reality is never perfect,  
64 they avoid difficulties inherent to *in vivo* studies such as costs, ethical considerations, technical  
65 complexity and variability. *In vitro* systems are various, leading to a diversity of protocols and  
66 physiological relevance levels. Dynamic models consist of different compartments through which the

67 studied food passes while the digestive juices are dynamically added. In some cases, mechanical devices  
68 are also incorporated in order to mimic the breakdown of foods. Even though these dynamic models are  
69 based on *in vivo* digestion, their use is complex, mostly suitable for liquid foods, and involves  
70 complicated engineering and high costs. On the other hand, cost effectiveness and good adaptability to  
71 the needs of the studied foods are the main advantages of static *in vitro* systems. Their *in vivo* digestion  
72 equivalence is nevertheless a drawback. Moreover, as they can be easily set up in most laboratories, a  
73 great number of protocols have been proposed. This has raised the need for harmonization of the key  
74 parameters (transit times, pH, enzymes used and their activities), a work that has been undertaken during  
75 the INFOGEST cost action and which has recently led to the publication of an international consensus  
76 (Minekus et al., 2014).

77 In association with static systems, the pH-stat titration method is a classical approach to monitor the  
78 intestinal phase of *in vitro* digestions. It consists in maintaining constant the pH of a food in contact  
79 with a digestive fluid mixture, whereas the enzyme-substrate reaction would normally modify it.  
80 Therefore, the quantity of titrant added during the experiment versus time is directly related to the  
81 production of hydrolyzed species. The method is easy to set up and directly provides the dynamics of  
82 the reaction. pH-stat is most often used to measure the progress of the lipolytic reaction (Day et al.,  
83 2014; Li & McClements, 2014), but can also be used to monitor the digestion of protein solutions or  
84 gels. To our knowledge, the simultaneous study of lipolysis and proteolysis with pH-stat has not been  
85 proposed yet.

86 Indeed, lipids and proteins are generally associated in real foods. Lipids are most often consumed in the  
87 form of oil in water emulsions (milk, sauces...). In such systems, proteins can be found in the aqueous  
88 continuous phase but also at the interface. The structural elements of an emulsion-type food matrix can  
89 affect its digestion behavior. For instance, the size of the oil droplets is a major parameter governing the  
90 kinetics of lipolysis (Armand et al., 1999; Giang et al., 2015). Lipolysis is an interfacial reaction.

91 Therefore, the rate of the reaction increases with the droplet surface area, i.e. smaller droplet sizes.  
92 Formulation and process conditions govern the droplet sizes in the emulsion, but transformations during  
93 digestion can also promote destabilization leading to a decrease in oil/water interface area (Clifton et  
94 al., 2011; Day et al., 2014). By controlling the emulsion stability against flocculation and coalescence,  
95 the nature of the interfacial layer is therefore also of importance for lipid digestion. Whey proteins can  
96 be used to achieve good stability of emulsions in gastric conditions (Clifton et al., 2011; Mantovani,  
97 Cavallieri, Netto, & Cunha, 2013). These proteins are reported to facilitate lipolysis compared to small  
98 surfactants, since they are subject to conformational changes through adsorption which can promote co-  
99 lipase anchorage and displacement action of bile salts (Mun, Decker, & McClements, 2007; Nik, Wright,  
100 & Corredig, 2010). Secondly, the physical state at a macroscopic scale of the continuous phase is an  
101 important parameter as liquid foods are prone to transiting through the stomach and intestine more  
102 rapidly than solid ones (J. E. Norton et al., 2014). Moreover, at a microscopic scale, whey proteins allow  
103 variations in the microstructure of the continuous phase. Their globular structure is sensible to heat and  
104 pH leading to various aggregated gel structures depending on gelation parameters. The sensitivity of  
105 whey proteins to hydrolysis is modulated by process conditions and is modified compared to native  
106 proteins (Macierzanka et al., 2012; T. K. Singh, Singh, Øiseth, Lundin, & Day, 2014).

107 The aim of this study was to develop a simple and robust method to assess the effects of the structures  
108 of complex food matrices on digestion. The association of a static *in vitro* digestion based on the  
109 INFOGEST protocol (Minekus et al., 2014) and a pH-stat method is proposed. The approach was used  
110 to investigate the digestion behaviors of two emulsion-type food matrices of identical compositions (10  
111 wt% oil, 15 wt% whey proteins) but with different structures at the macroscopic and microscopic scales.  
112 Results are discussed in relation with the structural effects of the matrices on the kinetics and final  
113 extents (degrees of hydrolysis) of both lipolysis and proteolysis.

## 114 **2 Materials and Method**

### 115 **2.1 Materials**

116 Rapeseed oil (Fleur de Colza, Lessieur, France) was purchased from a local supermarket. Whey protein  
117 isolate (WPI) (Prolacta 80) was purchased from Lactalis, France. The protein content was 72.9 wt% on  
118 dry powder measured by the Kjeldahl method (Nx6.25) in triplicate. Pepsin (P6887), pancreatin  
119 (P1750), pancreatic lipase (L3126) and bile extract (B8631) were all of porcine origin and obtained from  
120 Sigma-Aldrich, France. The enzyme activities and bile salt concentrations in the bile extracts were  
121 measured according to the assays detailed in Minekus et al. (2014). All other materials were standard  
122 analytical grade. Water was Milli-Q water.

### 123 **2.2 Preparation of food matrices**

124 Liquid-emulsions (LE) were prepared as follows. 15 g of whey proteins (WP) were dispersed in 50 g of  
125 water and allowed to rehydrate under continuous stirring at room temperature for at least an hour. 10 g  
126 of rapeseed oil were then added with water to achieve a final weight of 100 g. A coarse emulsification  
127 was made using a rotor-stator homogenizer (Polytron PT3100D) for 5 min at 10,000 rpm. This coarse  
128 emulsion was then treated with ultra-sounds for 10 min (10 s on/off cycles) in order to further reduce  
129 the size of the oil droplets (Bioblock Ultrasonic Processor 20 kHz, 130 W). During the two  
130 emulsification processes, the temperature within the sample was maintained below 30°C using an ice  
131 bath. The final emulsion contained 15 wt% of whey proteins and 10 wt% of rapeseed oil.

132 Solid-emulsions (SE) were prepared as follows. 0.24 g of WP were dispersed in 60 g of water and  
133 allowed to rehydrate under continuous stirring at room temperature for at least an hour. 24 g of rapeseed  
134 oil were then added with water to achieve a final weight of 80 g and a coarse emulsion was made using  
135 the rotor-stator homogenizer for 5 min at 10,000 rpm. The emulsion was thereafter heated at 70°C for 5

136 min to allow a certain degree of denaturation of proteins adsorbed at the interface of oil droplets. It was  
137 then mixed with a more-concentrated WP solution (22.33 wt%) in order to achieve final concentrations  
138 of 15 wt% of whey protein and 10 wt% of rapeseed oil. The emulsion was finally poured into 40 mL  
139 plastic cylindrical containers subsequently closed, immersed in a water bath, and heated for 30 min at  
140 80°C to produce a hard gel.

141 In order to estimate the respective contributions of proteolysis and lipolysis from the pH-stat signal,  
142 matrices only made of the continuous phases of the emulsions were also prepared and digested. The  
143 liquid proteinic continuous phase matrix (LCP) therefore consisted in a 15 wt% native whey protein  
144 solution while the solid proteinic continuous phase matrix (SCP) was made by heating LCP at 80°C for  
145 30 min.

### 146 **2.3 Characterization of matrices**

147 *Granulometry*: the oil droplet size distribution of the liquid emulsion was measured using laser light  
148 scattering (Mastersizer 2000, Malvern, France) with 1.47 as the refractive index of the oil and 1.33 as  
149 the refractive index of the dispersant (water). An absorption value of 0.001 was chosen for the optical  
150 properties of the emulsion. The volume-weighted mean diameter was calculated using  $d_{4,3}$  ( $d_{4,3} =$   
151  $\sum n_i d_i^4 / \sum n_i d_i^3$ ).

152 *Confocal microscopy*: solid (SE) and liquid (LE) matrices were observed with the use of confocal laser  
153 scanning microscopy (TCS SP2 AOBS by Leica, Solm, Germany) equipped with two He-Ne lasers with  
154 excitation wavelengths of 543 nm and 633 nm. A labelling protocol (Huc et al., 2014) was performed  
155 on lipids with the Bodipy 665/676 nm marker (Invitrogen, Carlsbad, NM, USA) and on proteins with the  
156 DyLight 488 nm marker (Thermo Fisher Scientific, Waltham, MA, USA). Images shown in this paper  
157 correspond to superimpositions of images of the same area observed separately with the two markers.

158 *Gel rheology*: thermal gelation was also characterized using a rheometer (MCR 301, Anton Paar) fitted  
159 with a Couette geometry ( $R_{\text{cup}}/R_{\text{cylinder}}=1.085$ ). The following sequences defined by the process used for  
160 solid-emulsion were performed: a linear temperature ramp from 30 to 80 °C at 3°C/min, a stabilization  
161 at 80°C for 30 min, a cooling back down to 30°C at 1°C/min, then a final stabilization of the temperature  
162 at 30°C for 20 min. The shear storage modulus at 0.1 % deformation with 1 Hz frequency was measured  
163 all along.

#### 164 **2.4 *In vitro* digestion protocol**

165 *In vitro* digestion experiments were carried out in a 50 mL bottle bathing in a jacketed beaker filled with  
166 water that was maintained at 37°C by heat water circulation in the double wall. The whole set was  
167 mounted on a magnetic stirrer (375 rpm).

168 *Electrolytes adjustment*: the digestion protocol used follows the recommendations given by Minekus et  
169 al. (2014) but an adaptation in the composition of the electrolyte solutions was needed. Indeed,  
170 experiments were first conducted by strictly following the protocol recommendations, but when trying  
171 to perform pH-stat analyses during the intestinal phase the measured pH actually increased instead of  
172 decreasing. As shown in Figure 1 (squares), the same phenomenon was observed when the simulated  
173 intestinal fluid electrolyte solution alone (eSIF) was placed in an open beaker at the concentration used  
174 during an intestinal digestion. The pH was continuously increasing above 7, while gas bubbles appeared  
175 on the glass surfaces of the pH probe and the vessel. On the contrary, when replacing  $\text{NaHCO}_3$  by  $\text{NaCl}$   
176 (circles in Figure 1), pH remained stable at 7. Following INFOGEST guidelines,  $\text{NaHCO}_3$  is present at  
177 85 mM, which corresponds to 7.14 g/L, and is the major contributor to hydrogenocarbonates in the final  
178 solution. This concentration is much higher than the solubility limit of  $\text{CO}_2$  (1.6 g/L at 20°C). Being in  
179 contact with the ambient atmosphere with the pH-stat setting, the  $\text{CO}_2$  concentration is therefore out of  
180 equilibrium and is rejected in its gaseous form, leading to a basification of the milieu. In all prepared

181 solutions (oral, gastric and intestinal) of the present study,  $\text{NaHCO}_3$  was therefore replaced by  $\text{NaCl}$  at  
182 the same molar ratio in order to maintain the same ionic strength.

183 *Gastro-intestinal digestion:* apart from this salt replacement ( $\text{NaCl}$  instead of  $\text{NaHCO}_3$ ) the protocol  
184 used was the same as in Minekus et al. (2014). Briefly, 5 g of food matrix were mixed with 5 mL of  
185 simulated salivary fluid (SSF) with no salivary  $\alpha$ -amylase (no starch in the matrices). For solid  
186 matrices, they were artificially grinded with a domestic kitchen food chopper (Braun Turbo 600 W type  
187 4191) during 3 s to produce pieces of solid gel ranging from 3 to 5 mm beforehand. For liquid matrices,  
188 the oral phase was only carried out for proper electrolyte concentrations and matrix dilution purposes.  
189 A few minutes were taken to reach temperature equilibrium at  $37^\circ\text{C}$  before proceeding to the gastric  
190 phase. To launch the gastric phase, 10 mL of simulated gastric fluid (SGF) were added to the mixture.  
191 It consisted of SGF electrolyte solutions (eSGF), pepsin solution to achieve a 2,000 U/mL activity in  
192 the final mixture, and  $\text{HCl}$  1 N to lower pH to 3. The gastric phase was kept running for 2 h. Finally, 20  
193 mL of simulated intestinal fluid (SIF) were added as the pH-stat titration was switched on. It consisted  
194 of SIF electrolyte solutions (eSIF), bile extract solution (10 mM bile salts in the final mixture),  
195 pancreatin added with pancreatic lipase (100 U/mL trypsin activity and 2,000 U/mL lipase activity in  
196 the final mixture) and  $\text{NaOH}$  1 N to adjust pH to 7. The intestinal phase was also 2 h long.

## 197 **2.5 pH-stat monitoring for the intestinal proteolysis and lipolysis**

198 As detailed in section 2.6 and 2.7, lipolysis and proteolysis performed by pancreatic enzymes lead to  
199 the release of protons, and hence to a decrease in pH. To monitor the kinetics of the reactions, an  
200 automatic titration unit (Titrino 7000, VWR, France) with a pH-stat programming to maintain the pH of  
201 the mixture at 7 was used with  $\text{NaOH}$  0.1 N as the titrant solution. All pH-stat titrations were carried  
202 out in triplicates using a data acquisition frequency of 1 s.

203 Besides, 6 h long experiments were performed on the intestinal digestive mixture alone, without any  
204 added substrate, to determine whether the hydrolysis coming from the auto-digestion of the digestive  
205 fluids could be neglected. Results showed that this was not the case as there was a progressive addition  
206 of 0.420 mL of NaOH during the 2 h of intestinal phase (data not shown). As a conclusion, special care  
207 should be taken with such digestion protocol because auto-digestion of digestive fluids can contribute  
208 to the signal measured with pH-stat. In the present study, this contribution was taken into account for  
209 proper calculations of the degrees of hydrolysis.

## 210 **2.6 Degree of Proteolysis**

211 During the hydrolysis of a peptide bond, one carboxylic group is produced along with one  $\alpha$ -amino  
212 group. According to their low pK values, carboxylic groups release their proton at pH 7, which are  
213 titrated by NaOH during the pH-stat experiment. However, the co-produced  $\alpha$ -amino group show pK  
214 values of about 7.4 at 37°C (Adler-Nissen, 1986) and may therefore consume protons to form  
215 ammonium groups. In the latter case, the proton captured by the  $\alpha$ -amino group therefore counteracts  
216 the one released by the carboxylic group and nothing is measured by titration (Nielsen, 1997). According  
217 to these phenomena, conversion from volumes of NaOH added into degree of hydrolysis ( $DH_{protein}$ , in  
218 %) can be calculated as follows (Asselin, Hébert, & Amiot, 1989; Spellman et al., 2003):

$$DH_{protein} = 100 \times \frac{V(NaOH) \times N(NaOH)}{\alpha(RNH_2) \times m(protein) \times h_{tot}} \quad (1)$$

219 where  $V(NaOH)$  is the volume (mL) of NaOH consumed during the titration,  $N(NaOH)$  is the NaOH  
220 normality (Eq/L),  $m(protein)$  is the protein mass (g),  $h_{tot}$  is the number of peptide bonds in the protein  
221 substrate (= 8.8 meqv/g for whey proteins (Spellman et al., 2003)) and  $\alpha(RNH_2)$  is the mean degree of  
222 dissociation of  $\alpha$ -amino groups, which can be calculated as follows:

$$\alpha(\text{RNH}_2) = \frac{10^{(pH-pK)}}{1 + 10^{(pH-pK)}} \quad (2)$$

223 where pK is the average dissociation constant for the  $\alpha$ -amino groups liberated during hydrolysis.

224 The value of pK depends on several parameters such as temperature, peptide chain length or the nature  
225 of the terminal amino acid. It can therefore vary depending on the protein substrate and enzymes used.

226 To get a proper estimate of the pK value in our conditions, complementary experiments using the OPA  
227 (ortho-phthalaldehyde) method were therefore conducted.

228 *Quantification of DH using OPA:* Degrees of hydrolysis were measured on LCP at the end an intestinal  
229 phase (with no preceding gastric phase) using the protocol proposed by Spellman et al. (2003) except  
230 that no SDS were added. Briefly, this method is based on the detection at 340 nm of a complex formed  
231 between the  $\alpha$ -amino groups of peptides and OPA (ortho-phthalaldehyde) in the presence of N-acetyl-  
232 L-cysteine. The difference of absorbance between the hydrolyzed and the corresponding unhydrolyzed  
233 samples therefore provide the number of  $\alpha$ -amino groups produced during the proteolytic reaction. In  
234 this study, a UV-Vis Spectrophotometer (Evolution 201, Thermo Scientific) was used and the  
235 unhydrolyzed samples were prepared by mixing LCP with heat-treated (90°C – 10 min) SIF. By  
236 comparing the DH measured by the OPA method for LCP to the corresponding volume of added NaOH  
237 with pH-stat, a mean pK of the  $\alpha$ -amino groups of about 7.85 could be estimated, which leads to a value  
238 of 0.12 for  $\alpha(\text{RNH}_2)$  (Table 1). Note that the OPA method cannot be used to determine DH values with  
239 solid matrices because of sampling difficulties. For SCP, the degree of hydrolysis was therefore  
240 estimated using Eq. 1 with an  $\alpha(\text{RNH}_2)$  value of 0.12.

## 241 **2.7 Degree of Lipolysis**

242 When fully digested, one triglyceride molecule liberates two free fatty acids (FFA) coming from

243 positions sn-1 and sn-3 as well as the sn-2-monoglyceride. Two moles of NaOH are therefore required  
244 to neutralize one mole of digested triglyceride. However, as for of proteins, all the FFA released are not  
245 necessarily readily ionized depending on the pH of the milieu and the pK of the fatty acids. In a similar  
246 way as previously described for proteolysis, the degree of hydrolysis for lipids ( $DH_{lipid}$ , in %) can be  
247 calculated as follows:

$$DH_{lipid} = 100 \times \frac{V(NaOH) \times N(NaOH) \times M(lipid)}{\alpha(FFA) \times m(lipid) \times 2} \quad (3)$$

248 where  $V(NaOH)$  and  $N(NaOH)$  have the same meaning as in (Eq. 1),  $m(lipid)$  is the oil mass (g),  
249  $M(lipid)$  is the molecular weight (g/mol) of the triglycerides in the oil (930 g/mol in this study), and  
250  $\alpha(FFA)$  is the mean degree of dissociation of FFA carboxylic groups.

251 To estimate the value taken by  $\alpha(FFA)$  in our experimental conditions, complementary 6h30-long  
252 intestinal digestions were performed on reduced quantities (0.5 g) of an emulsion with 10 wt% rapeseed  
253 oil and 0.1 wt% WP in order to reach 100 % liberation of fatty acids (controlled by the appearance of a  
254 real plateau during pH-stat measurements). Taking into account the auto-digestion of pancreatic juice,  
255  $\alpha(FFA)$  was estimated to be 0.54 (Table 1). Note that this value corresponds to a pK of about 6.9 (Eq.  
256 2), which is in good agreement with the reported pK values for long chain fatty acids (Fernandez et al.,  
257 2008).

## 258 **3 Results and Discussion**

### 259 **3.1 Characterization of the designed emulsions**

260 Confocal microscopy images and droplet size distributions of the two emulsions are presented in Figure  
261 2. As expected, oil droplets are bigger in the solid emulsion (SE) and seem more poly-dispersed (Figure  
262 2B and 2D) than in the liquid emulsion (LE) (Figure 2A and 2C). Mean droplet diameters were  $0.748 \pm$   
263  $0.055 \mu\text{m}$  for LE and  $19.842 \pm 0.569 \mu\text{m}$  for the SE emulsion before the first heat treatment (Figures 2C  
264 and 2D, respectively). Droplet size changes in SE after the first heat treatment were controlled using  
265 laser granulometry and found not significant. In LE, a uniform green background can be seen, suggesting  
266 a homogenous protein solution continuous phase (Figure 2A). On the contrary, the continuous phase  
267 made of proteins shows irregularities in the SE structure (Figure 2B), suggesting a non-homogenous  
268 gelation process during the second heat treatment (30 min at  $80^\circ\text{C}$ ). The rheology test performed on the  
269 SE gave the value of  $58 \pm 1 \text{ kPa}$ , corresponding to a quite high hardness. As a conclusion, the two  
270 designed matrices were different in both microstructure (droplet diameter ratio  $\text{SE} / \text{LE} = 26.5$ ) and  
271 macrostructure (liquid vs solid).

### 272 **3.2 Digestion of the liquid and solid emulsions**

273 The results from pH-stat experiments during the intestinal digestion of the liquid and solid emulsions  
274 are shown in Figure 3A. Both kinetics are similar in shape, with a fast rate at the beginning of the titration  
275 followed by a progressive slowing down leading to a pseudo-plateau that was reached earlier for LE ( $\sim$   
276  $0.1 \text{ h}$ ) than SE ( $\sim 1 \text{ h}$ ). The final volume of added NaOH is also similar for both matrices (about  $9 \text{ mL}$ ).  
277 A semi-log scale (Figure 3B) was also used to give a complementary view of the data at both short and  
278 long digestion times. It confirms the faster liberation of titrated elements during the first minutes ( $6.3$   
279  $\text{mL}$  within  $0.1 \text{ h}$ ) for LE. Then the kinetics slow down to reach  $8.9 \text{ mL}$  at the end of the  $2 \text{ h}$  of digestion  
280 but do not tend to a plateau, indicating that the reactions were not ended at this time. The SE curve

281 shows a rather reduced rate of hydrolysis at the beginning of the digestion. It starts to increase at a  
282 smaller rate than the LE curve and finally crosses it after 23 min. At the end of the 2 h, the SE curve has  
283 attained 9.5 mL Like for LE, a real plateau is not reached after 2 h.

284 The different shapes of the titration curves can be related to the different physical states of the matrices.  
285 Protein molecules and oil droplets are moving freely in LE. Therefore, both substrates are rapidly  
286 exposed to the enzyme actions. On the contrary, gel pieces were still visible for SE after 2 h of gastric  
287 phase, implying that oil droplets were still entrapped in the proteinic network of gel pieces for this  
288 matrix. Therefore, enzymes have to diffuse into the SE gel pieces before finding their substrate, which  
289 leads to slower digestion kinetics. Luo, Boom, & Janssen (2015) have also compared *in vitro* gastric  
290 digestions of WP solutions and gels and explain similar behaviors by a “zipper” type mechanism for the  
291 proteins-in-solution reaction (fast initial hydrolysis followed by a steadier stage) opposed to a “one-by-  
292 one” mechanism for proteinic gels (slower initial rate followed by a more-sustained trend).

### 293 **3.3 Digestion of the proteinic continuous phase matrices (SCP and LCP)**

294 In order to estimate the proteolysis contribution during pH-stat experiments performed on SE and LE,  
295 lipid-free matrices with the same structures were studied. This implicitly supposes that the absence of  
296 oil droplets does not significantly influence the kinetics of proteolysis and the structure of the protein  
297 network. Under these hypotheses, one can expect the overall trends and final extents of digestion to be  
298 largely unchanged.

299 It can first be noted that, as for SE, gel pieces of SCP were almost not modified in shape at the end of  
300 the gastric phase, implying limited pepsin hydrolysis and the persistence of solid state effects on  
301 digestion. The pH-stat results obtained during the intestinal digestion of the liquid and solid proteinic  
302 continuous phase matrices (LCP and SCP) are presented in Figures 4A and 4B on a linear and semi-log  
303 scale, respectively. Both curves draw similar trends to the ones shown in Figure 3 with a faster reaction

304 rate in the first minutes of digestion, and similar inflexion points and slowdowns. This result validates  
305 the major contribution of the continuous phase's physical state on hydrolysis kinetics. In this case,  
306 however, a real plateau is reached for both LCP and SCP (Figure 4A and B), indicating that the  
307 proteolysis reactions were finished within the 2h of intestinal digestion. The major difference between  
308 the liquid and solid matrices lies in the final levels of NaOH added which, after 2 h, were of 4.2 mL and  
309 6.5 mL, respectively. This means that the contribution of proteolysis to the overall pH-stat signal  
310 measured during digestion of the lipo-proteinic emulsions was important, and represented about 50 %  
311 and 70 % of the added NaOH for LE and SE, respectively.

312 At the end of the intestinal phase, the degree of hydrolysis was estimated to be  $52 \pm 2$  % for LCP and  
313  $80 \pm 1$  % for SCP (Table 1). These results are in good agreement with the recent studies of Picariello et  
314 al. (2015) and Egger et al. (this issue) who reported values of about 60 % using the INFOGEST *in vitro*  
315 protocol to digest dairy proteins. Besides, the greater final level reached with SCP than LCP can  
316 probably be attributed to the greater sensitivity of denatured whey proteins to hydrolysis by intestinal  
317 proteases. This finding is indeed consistent with the literature (Macierzanka et al., 2012; T. K. Singh et  
318 al., 2014).

### 319 **3.4 Estimation of the lipolytic kinetics**

320 The contributions of the lipolysis reactions to the SE and LE kinetics were approximated by subtracting,  
321 point by point, the pH-stat data collected with proteinic continuous phase (LCP and SCP) from the ones  
322 collected with emulsions (LE and SE). Results are presented in Figure 5 (linear and semi-log). The curve  
323 shapes are similar to the ones obtained for the digestions of emulsions (LE, SE) and proteinic continuous  
324 phases (LCP, SCP) (Figures 3 and 4), meaning a faster rate in the first minutes followed by slower  
325 kinetics after an inflexion point. Comparatively to Figure 4 though, the final amount of added NaOH  
326 obtained with the liquid matrix is higher than the solid one (4.7 mL vs. 2.9 mL). Moreover, a real plateau

327 was not reached after 2 h for both curves, as previously observed with LE and SE (Figure 3). This  
328 demonstrates that the kinetics of lipolysis are slower than the kinetics of proteolysis (Figure 4).

329 Using Equation 3, a final degree of lipolysis of  $81 \pm 10$  % and of  $51 \pm 6$  % for the lipids of LE and SE  
330 were found, respectively (Table 1). The order of magnitude of these values are in good accordance with  
331 the literature (Giang et al., 2015; Li & McClements, 2010; Williams et al., 2012). Besides, the higher  
332 level of lipolysis for LE than SE may be related to the physical state of the continuous phase and to the  
333 sizes of the oil droplets in the emulsions. Indeed, lipids are readily available for hydrolysis as soon as  
334 enzyme adjunction has been made for LE, whereas pancreatic lipase have to diffuse into the gel pieces  
335 and/or oil droplets must first be liberated from the protein gel network for the reaction to take place.  
336 Moreover, the faster rate of titration for LE may also be related to the smaller sizes of oil droplets  
337 dispersed in it. Lipolysis is an interfacial enzymatic reaction; so, for the same amount of lipids, the  
338 smaller the droplets, the larger the oil/water interfacial area, and the faster the reaction.

339 The fact that lipolysis is not finished at the end of the experiments is a classical result with long-chain  
340 triglycerides (Clifton et al., 2011; Giang et al., 2015; Li & McClements, 2010). The slowdown in the  
341 kinetics could be due to an inhibition of the reaction by the lipolysis products (Mun et al., 2007; Pafumi,  
342 2002) or a certain degree of coalescence that decreased the interface area available to the lipase action  
343 (Giang et al., 2015; Clifton et al., 2011; Day et al., 2014).

#### 344 **4 Conclusion**

345 This study was aiming at developing a methodology to compare structure-related effects of model lipo-  
346 proteinic foods on their digestion. The feasibility and interest of using the pH-stat method in association  
347 with the INFOGEST *in vitro* digestion protocol was proved. It resulted in a simple and quantitative  
348 method that allows a continuous monitoring of the intestinal digestions of both proteins and lipids. This  
349 method is a very valuable add-on to the INFOGEST protocol because it makes possible to follow *in*  
350 *vitro* digestion in real time without the requirement of samplings at specific time points.

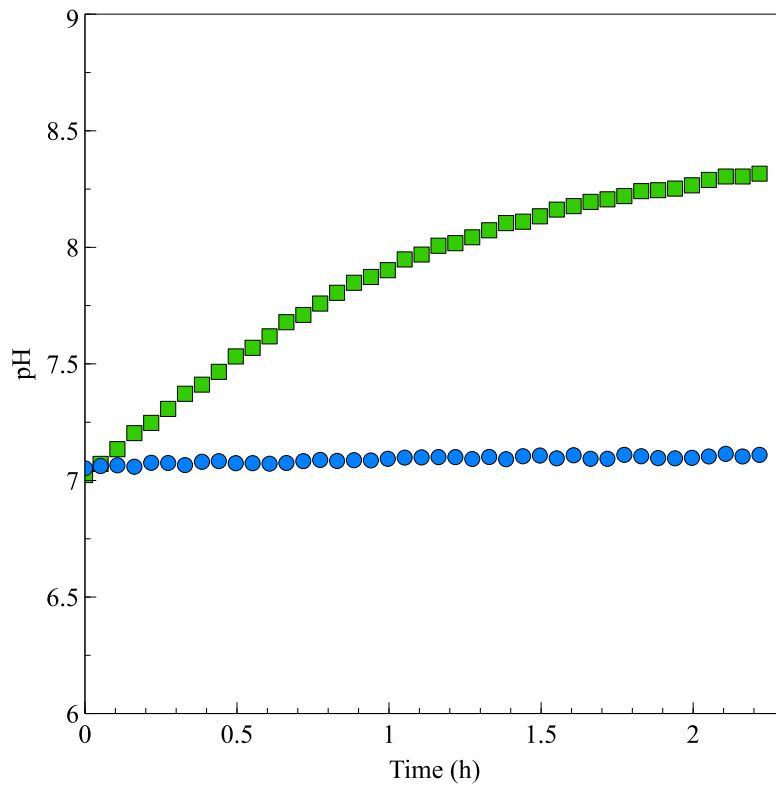
351 Applying this method to model emulsion-type food matrices with the same compositions but different  
352 structures allowed observing differences in their digestion kinetics and extents for both proteins and  
353 lipids. The physical state of the continuous phase and the native *versus* denatured state of whey proteins  
354 were found to be important factors of the overall dynamics for both protein and lipid digestion.

355

356

#### 357 **Acknowledgments**

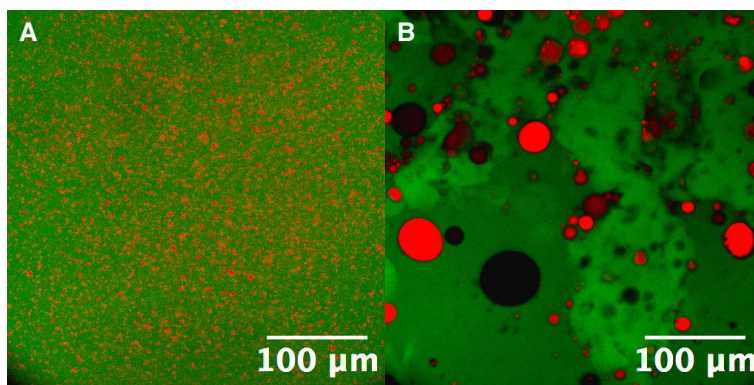
358 This work received support from the French National Research Agency under the "Investissements  
359 d'Avenir" program (reference No. ANR-11-IDEX-0003-02). The author would like to thank Thomas  
360 Cattenoz (UMR782 GMPA, Thiverval-Grignon, France) for his help with the setting of the digestion  
361 protocol. A special thank to Véronique Bosc (UMR1145 GENIAL, Massy, France) for sharing her  
362 knowledge of the emulsification process and to Gabrielle Moulin and Delphine Huc for their help for  
363 confocal microscopy observations. The authors are involved in the Food and Agriculture COST  
364 (European Cooperation in Science and Technology) Action FA1005 'Improving health properties of  
365 food by sharing our knowledge on the digestive process (INFOGEST)'.



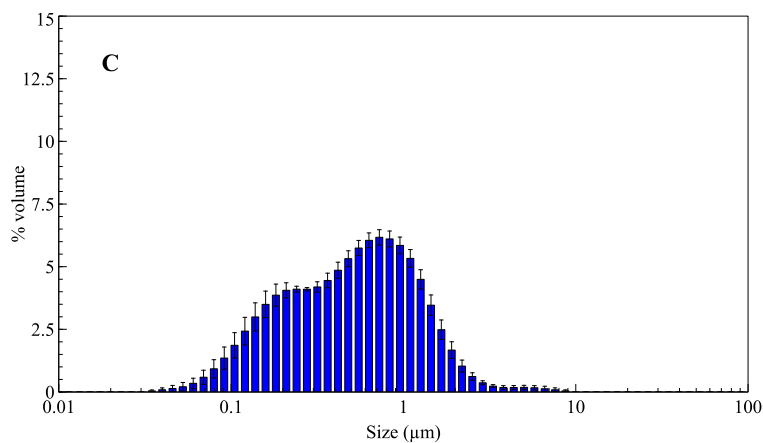
366  
367 **Figure 1:** pH evolution of the electrolyte solution used for intestinal phase (eSIF) when placed in an  
368 open beaker: (squares) eSIF prepared with respect to the *in vitro* digestion recommendations proposed  
369 by Minekus et al. (2014), and (circles) eSIF in which NaHCO<sub>3</sub> was replaced by NaCl.

370

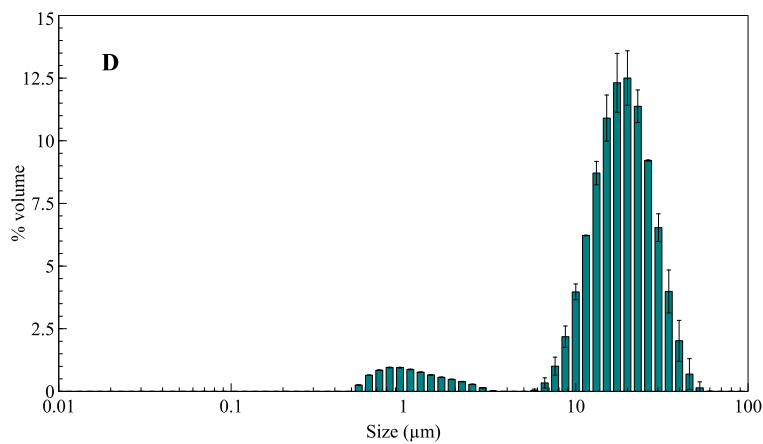
371



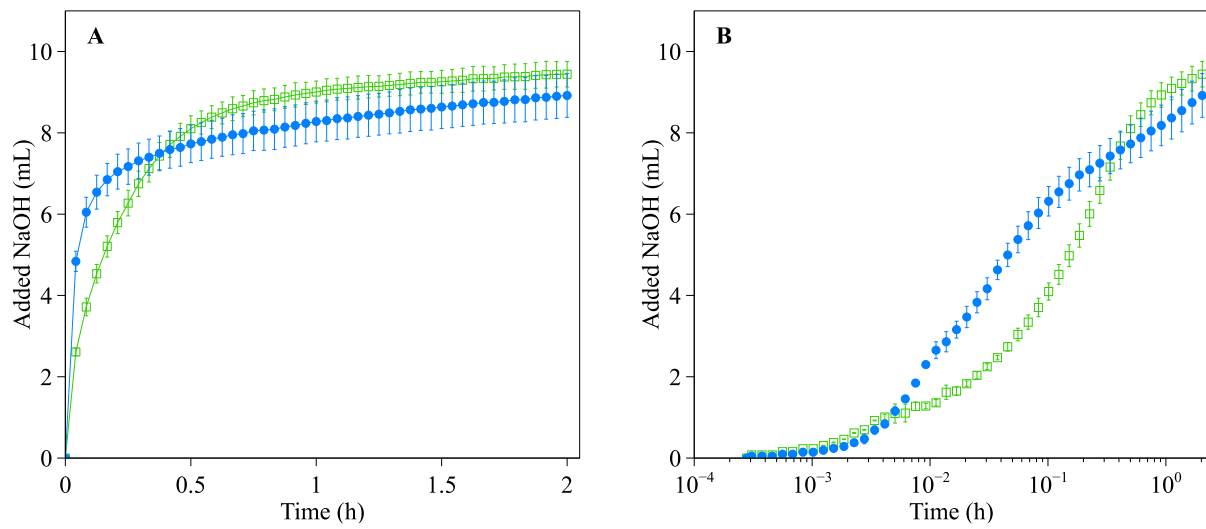
372



373



374 **Figure 2:** Characterization of the microstructures of emulsions containing 15 wt% rapeseed oil and 10  
375 wt% whey proteins. Confocal micrographs of the liquid emulsion (A) and the solid emulsion (B) at  
376 magnification x40 (lipids appear in red and proteins in green). Laser light scattering determination of  
377 the sizes of the oil droplets in the liquid emulsion (C) and in the emulsion prepared before heat treatment  
378 of the solid matrix (D).



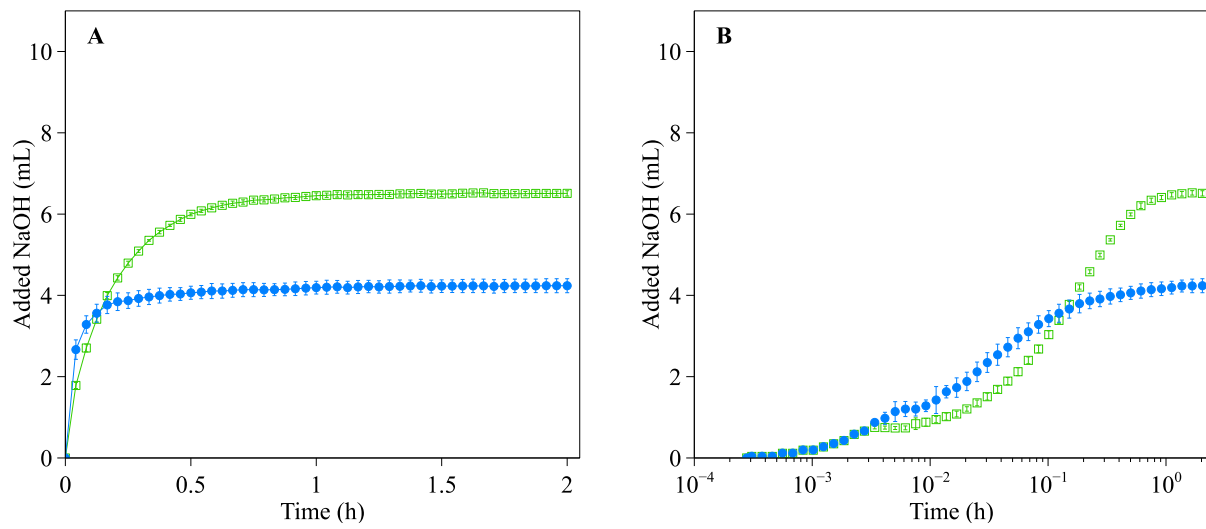
379

380 **Figure 3:** pH-stat profiles measured during the intestinal phases of digestion for the liquid emulsion

381 (filled circles) and the solid emulsion (open squares) on linear (A) and semi-log (B) scales. Values are

382 means  $\pm$  SD over 3 replicates.

383

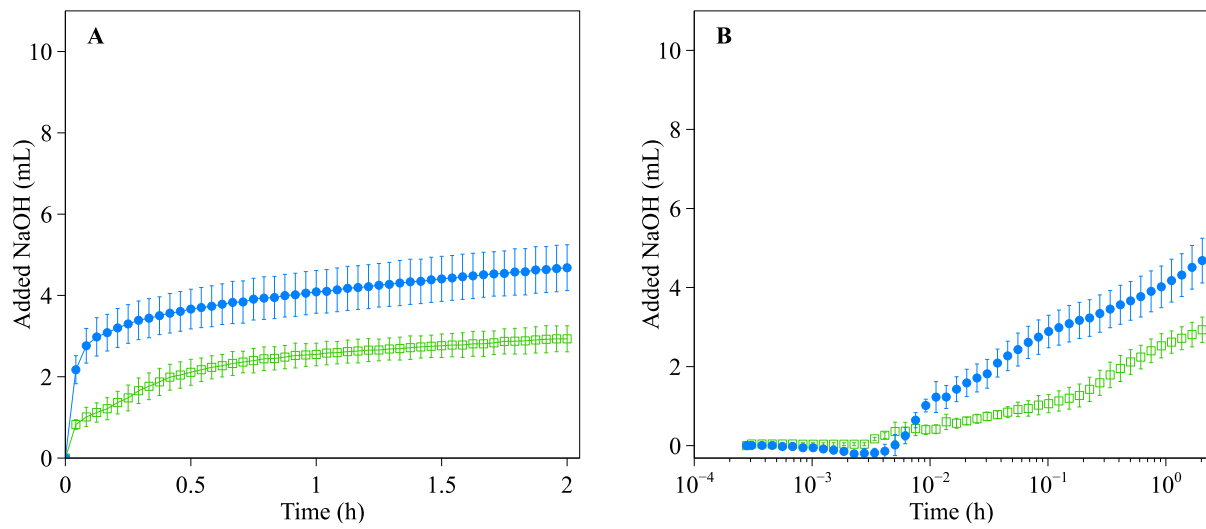


384

385 **Figure 4:** pH-stat profiles measured during the intestinal phases of digestion for the liquid proteinic

386 continuous phase matrix (filled circles) and the solid proteinic continuous phase matrix (open squares)

387 on linear (A) and semi-log (B) scales. Values are means  $\pm$  SD over 3 replicates.



388

389 **Figure 5:** pH-stat profiles of the lipolysis during the intestinal phases of digestion estimated by  
 390 subtracting Figure 4 from Figure 3, for lipids in the liquid emulsions (filled circles) and in the solid  
 391 emulsions (open squares), on linear (A) and semi-log (B) scales. Values are means  $\pm$  SD over 3  
 392 replicates.

393

394 **Table 1:** Degree of hydrolysis at the end of 2h of intestinal digestion and mean degree of dissociation  
395 of the peptide  $\alpha$ -amino groups and fatty acid carboxyl groups.

396

397

<b>Nutrients</b>	<b>Matrix</b>	<b>Degree of hydrolysis (%)</b>	<b>Degree of dissociation (correction factor)</b>
<b>Proteins</b>	Liquid	$52 \pm 2$	0.12 ( $\alpha$ in equation 1)
	Solid	$80 \pm 1$	
<b>Lipids</b>	Liquid	$81 \pm 10$	0.54 ( $\alpha$ in equation 3)
	Solid	$51 \pm 6$	

398 **References**

- 399 Adler-Nissen, J. (1986). *Enzymic Hydrolysis of Food Proteins*. Elsevier Science Limited.
- 400 Armand, M., Pasquier, B., André, M., Borel, P., Senft, M., Peyrot, J., et al. (1999). Digestion and  
401 absorption of 2 fat emulsions with different droplet sizes in the human digestive tract. *The American*  
402 *Journal of Clinical Nutrition*, 70(6), 1096–1106.
- 403 Asselin, J., Hébert, J., & Amiot, J. (1989). Effects of In Vitro Proteolysis on the Allergenicity of Major  
404 Whey Proteins. *Journal of Food Science*, 54(4), 1037–1039. [http://doi.org/10.1111/j.1365-](http://doi.org/10.1111/j.1365-2621.1989.tb07938.x)  
405 2621.1989.tb07938.x
- 406 Clifton, P. M., Golding, M., Keogh, J., Wooster, T. J., Lundin, L., Xu, M., et al. (2011). Impact of gastric  
407 structuring on the lipolysis of emulsified lipids. *Soft Matter*, 7(7), 3513.  
408 <http://doi.org/10.1039/c0sm01227k>
- 409 Day, L., Golding, M., Xu, M., Keogh, J., Clifton, P. M., & Wooster, T. J. (2014). Tailoring the digestion  
410 of structured emulsions using mixed monoglyceride–caseinate interfaces. *Food Hydrocolloids*, 36,  
411 151–161. <http://doi.org/10.1016/j.foodhyd.2013.09.019>
- 412 Egger, L., Ménard, O., Delgado-Andrade, C., Alvito, P., Assunção, R., Balance, S. et al. (2015). The  
413 harmonized INFOGEST in vitro digestion method: From knowledge to action. *This issue*.
- 414 Fernandez, S., Rodier, J. D., Ritter, N., Mahler, B., Demarne, F., Carrière, F., & Jannin, V. (2008).  
415 Lipolysis of the semi-solid self-emulsifying excipient
- 416 Gelucire (R) 44/14 by digestive lipases. *Biochimica Et Biophysica Acta-Molecular and Cell Biology of*  
417 *Lipids*, 1781(8), 367–375. <http://doi.org/10.1016/j.bbalip.2008.05.006>
- 418 Giang, T. M., Le Feunteun, S., Gaucel, S., Brestaz, P., Anton, M., Meynier, A., & Trelea, I. C. (2015).  
419 Dynamic modeling highlights the major impact of droplet coalescence on the in vitro digestion  
420 kinetics of a whey protein stabilized submicron emulsion. *Food Hydrocolloids*, 43, 66–72.  
421 <http://doi.org/10.1016/j.foodhyd.2014.04.037>
- 422 Guerra, A., Etienne-Mesmin, L., Livrelli, V., Denis, S., Blanquet-Diot, S., & Alric, M. (2012).

- 423 Relevance and challenges in modeling human gastric and small intestinal digestion. *Trends in*  
424 *Biotechnology*, 30(11), 591–600. <http://doi.org/10.1016/j.tibtech.2012.08.001>
- 425 Huc, D., Mariette, F., Challos, S., Barreau, J., Moulin, G., & Michon, C. (2014). Multi-scale  
426 investigation of eyes in semi-hard cheese. *Innovative Food Science & Emerging Technologies*, 24,  
427 106–112. <http://doi.org/10.1016/j.ifset.2013.10.002>
- 428 Li, Y., & McClements, D. J. (2010). New mathematical model for interpreting pH-stat digestion profiles:  
429 impact of lipid droplet characteristics on in vitro digestibility. *Journal of Agricultural and Food*  
430 *Chemistry*, 58(13), 8085–8092. <http://doi.org/10.1021/jf101325m>
- 431 Li, Y., & McClements, D. J. (2014). Modulating lipid droplet intestinal lipolysis by electrostatic  
432 complexation with anionic polysaccharides: Influence of cosurfactants. *Food Hydrocolloids*, 35,  
433 367–374. <http://doi.org/10.1016/j.foodhyd.2013.06.011>
- 434 Luo, Q., Boom, R. M., & Janssen, A. (2015). Digestion of protein and protein gels in simulated gastric  
435 environment. *LWT-Food Science and Technology*. <http://doi.org/10.1021/jf60208a021>
- 436 Macierzanka, A., Böttger, F., Lansonneur, L., Groizard, R., Jean, A.-S., Rigby, N. M., et al. (2012). The  
437 effect of gel structure on the kinetics of simulated gastrointestinal digestion of bovine  $\beta$ -  
438 lactoglobulin. *Food Chemistry*, 134(4), 2156–2163.  
439 <http://doi.org/10.1016/j.foodchem.2012.04.018>
- 440 Mackie, A., & Macierzanka, A. (2010). Colloidal aspects of protein digestion. *Current Opinion in*  
441 *Colloid & Interface Science*, 15(1-2), 102–108. <http://doi.org/10.1016/j.cocis.2009.11.005>
- 442 Mantovani, R. A., Cavallieri, Â. L. F., Netto, F. M., & Cunha, R. L. (2013). Stability and in vitro  
443 digestibility of emulsions containing lecithin and whey proteins. *Food & Function*, 4(9), 1322–  
444 1331. <http://doi.org/10.1039/c3fo60156k>
- 445 Minekus, M., Alminger, M., Alvito, P., Ballance, S., Bohn, T., Bourlieu, N. C., et al. (2014). A  
446 standardised static in vitro digestion method suitable for food - an international consensus. *Food &*  
447 *Function*, 5(6), 1113–1124. <http://doi.org/10.1039/c3fo60702j>
- 448 Mun, S., Decker, E. A., & McClements, D. J. (2007). Influence of emulsifier type on in vitro digestibility  
449 of lipid droplets by pancreatic lipase. *Food Research International*, 40(6), 770–781.

- 450 <http://doi.org/10.1016/j.foodres.2007.01.007>
- 451 Nielsen, P. M. (1997). Functionality of Protein Hydrolysates. In *Food Proteins and Their Applications*  
452 (p. 694). Taylor & Francis.
- 453 Nik, A. M., Wright, A. J., & Corredig, M. (2010). Surface adsorption alters the susceptibility of whey  
454 proteins to pepsin-digestion. *Journal of Colloid and Interface Science*, 344(2), 372–381.  
455 <http://doi.org/10.1016/j.jcis.2010.01.006>
- 456 Norton, J. E., Wallis, G. A., Spyropoulos, F., Lillford, P. J., & Norton, I. T. (2014). Designing food  
457 structures for nutrition and health benefits. *Annual Review of Food Science and Technology*, 5(1),  
458 177–195. <http://doi.org/10.1146/annurev-food-030713-092315>
- 459 Pafumi, Y. (2002). Mechanisms of Inhibition of Triacylglycerol Hydrolysis by Human Gastric Lipase.  
460 *Journal of Biological Chemistry*, 277(31), 28070–28079. <http://doi.org/10.1074/jbc.M202839200>
- 461 Picariello, G., Miralles, B., Mamone, G., Sánchez-Rivera, L., Recio, I., Addeo, F., & Ferranti, P. (2015).  
462 Role of intestinal brush border peptidases in the simulated digestion of milk proteins. *Molecular*  
463 *Nutrition & Food Research*, 59(5), 948–956. <http://doi.org/10.1002/mnfr.201400856>
- 464 Singh, H., Ye, A., & Horne, D. (2009). Structuring food emulsions in the gastrointestinal tract to modify  
465 lipid digestion. *Progress in Lipid Research*, 48(2), 92–100.  
466 <http://doi.org/10.1016/j.plipres.2008.12.001>
- 467 Singh, T. K., Singh, T. K., Øiseth, S. K., Lundin, L., & Day, L. (2014). Influence of heat and shear  
468 induced protein aggregation on the in vitro digestion rate of whey proteins. *Food & Function*, 5(11),  
469 2686–2698. <http://doi.org/10.1039/c4fo00454j>
- 470 Spellman, D., McEvoy, E., O’Cuinn, G., & FitzGerald, R. J. (2003). Proteinase and exopeptidase  
471 hydrolysis of whey protein: Comparison of the TNBS, OPA and pH stat methods for quantification  
472 of degree of hydrolysis. *International Dairy Journal*, 13(6), 447–453.  
473 [http://doi.org/10.1016/S0958-6946\(03\)00053-0](http://doi.org/10.1016/S0958-6946(03)00053-0)
- 474 Turgeon, S. L., & Rioux, L.-E. (2011). Food matrix impact on macronutrients nutritional properties.  
475 *Food Hydrocolloids*, 25(8), 1915–1924. <http://doi.org/10.1016/j.foodhyd.2011.02.026>

476 Turgeon, S. L., Bard, C., & Gauthier, S. F. (1991). Comparaison de trois méthodes pour la mesure du  
477 degré d'hydrolyse de protéines laitières modifiées enzymatiquement. *Canadian Institute of Food*  
478 *Science and Technology Journal*, 24(1-2), 14–18. [http://doi.org/10.1016/S0315-5463\(91\)70013-8](http://doi.org/10.1016/S0315-5463(91)70013-8)

479 Williams, H. D., Sassene, P., Kleberg, K., Bakala-N’Goma, J.-C., Calderone, M., Jannin, V., et al.  
480 (2012). Toward the establishment of standardized in vitro tests for lipid-based formulations, part 1:  
481 method parameterization and comparison of in vitro digestion profiles across a range of  
482 representative formulations. *Journal of Pharmaceutical Sciences*, 101(9), 3360–3380.  
483 <http://doi.org/10.1002/jps.23205>

484